Internal Dynamics of Poly(Methylphenylsiloxane) Chains as Revealed by Picosecond Time Resolved Fluorescence†

Fernando B. Dias,‡ Joao C. Lima,‡,⊥ Inés F. Piérola,§ Arturo Horta,§ and Antonio L. Maçanita*,‡,||

Instituto de Tecnologia Química e Biológica (ITQB/UNL), Oeiras, Portugal, Department Fisicoquímica (CTFQ), Universidad a Distancia (UNED), Madrid, Spain, and Instituto Superior Técnico (IST/UTL), Lisboa, Portugal

Received: February 12, 2001; In Final Form: April 9, 2001

The dynamics of linear polymethylphenylsiloxane chains in dilute methylcyclohexane solution was probed with picosecond time-resolved fluorescence. Experiments were performed, for one monodisperse sample with an average number of skeletal bonds equal to 25, at temperatures covering a wide range (193−293 K). Triple exponential decays were observed at the monomer and excimer emission wavelengths. The three relaxation times were interpreted and full analyzed on the basis of a kinetic scheme, which involves three kinetically coupled species in the excited state: the excimer (E) and two different types of monomers (M_{nh} and M_h). The transition of these monomers to excimer occurs at different rates, M_{nh} by a fast transition (k_a), and M_h by a slower transition (k_u). Molecular dynamics simulations for the approach of two chromophores to the excimer configuration suggest that there are two time regimes that can be ascribed to these transitions. The fast one to unrestricted motions controlled just by local bond rotations at the level of a single dyad, and the slower one to retarded motions in which the local bond rotations of the dyad occur only after a delay time caused by the coupling of the dyad to the attached chain. The corresponding to theoretical reciprocal relaxation times are in qualitative agreement with the experimental relative values of k_a and k_u. These results reveal that the dynamics of dyads is influenced by the rest of the backbone, something that can be responsible for the generally complex excimer formation kinetics in polymers. The rates and activation energies of these two transition modes of the chain were measured: Many of the Si−O−Si double (synchronized) rotations leading to the approach of two neighbor phenyl rings to the close distance excimer configuration occur fast, as in a single diad, with $k_a(20\ °C) = 1.4 \times 10^{10}\ s^{-1}$ and $E_a = 2.2$ kcal mol^{-1}, but a few suffer a lag (like frozen in the nonexcimer configuration), due to retardation imposed by the polymer, giving the slower rate $k_u(20\ °C) = 1.2 \times 10^{9} s^{-1}$ and $E_u = 5.6$ kcal mol^{-1}. The fractions of "frozen" monomers, $\beta = 0.04$, of ground-state dimers, $\alpha = 0.05$, and the rate of energy transfer between "frozen" neighbor phenyl rings, $k_t = 5.6 \times 10^{8}\ s^{-1}$, were also measured. Steady state fluorescence results are accurately reproduced by using the proposed kinetic scheme and the parameters evaluated from time-resolved results.

Introduction

Silicones are materials whose applications are closely related to the molecular properties of the siloxane chain. The chain backbone is so flexible that to study its dynamics in nonviscous solutions, techniques working in the picosecond time range should be needed.[1] Fluorescence spectroscopy, and in particular monomer−excimer time-resolved emission, can be a useful tool to study polymer dynamics,[1−26] provided the usual complexity of decays found in polymers can be interpreted, analyzed, and translated to physically meaningful parameters. The usefulness of this tool is largest when such complexity (more information) is due to the forward process of forming the excimer, which is directly related to the chain dynamics.

We have previously studied intramolecular excimer formation between the phenyl groups of linear[10,15−17,20] poly(methylphenylsiloxane)s (PMPS*N*) and related systems[12−17] (Chart 1), using nanosecond time resolution. The fluorescence decays were indeed complex (sums of at least three exponentials), and we were unable to perform a complete analysis of the data.[20] These results were in contrast with our findings with the model dyad, 1,3-diphenyltetramethyldisiloxane (PMPS2), for which double exponential decays were measured in a wide range of temperatures.[20]

There are at least two possible causes, other than experimental problems, for multiple exponential decays. First, more than one class of excimers may be formed (e.g., excimers formed by two nearest-neighbor monomers (NNE), excimers formed by two next-to-nearest-neighbor monomers (NNNE)[22] or long range excimers), when these excimers are kinetically and/or structurally different. In this case, $N+1$ kinetically coupled species (one monomer and N excimers) will be present, and the decay laws of monomer and excimer will be sums of $N+1$ exponentials and not sums of two exponentials. The classical example of this situation is 1,3-(1,1-dipyrenyl)propane) where two excimers are present.[27]

Second, more than one class of kinetically different monomers

† This work was presented at the PP2000 in Costa do Estoril, Portugal, honoring Professor Ralph Becker's contributions.

‡ Instituto de Tecnologia Química e Biológica.

§ Department Fisicoquímica .

|| Instituto Superior Técnico.

⊥ Present address: Centro de Química Fina e Biotecnologia, FCT/UNL, Monte da Caparica, Portugal.

10.1021/jp010547f CCC: $20.00
Published on Web 06/05/2001

CHART 1

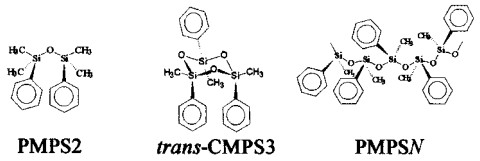

PMPS2 ***trans*-CMPS3** **PMPS*N***

may also exist. This may occur whenever there are groups of monomers that are separated by high energy barriers (sufficiently high to make of them kinetically distinct species). An extreme example of this situation is the case of the cyclic trisiloxane, 1,3,5-triphenyl-1,3,5-trimethyl-cyclotrisiloxane (CMPS3).[25] In the trans isomer of CMPS3 there are two classes of monomers: two monomers (down) and one "isolated monomer" (up). This monomer is unable to reach the excimer forming conformation, but it can transfer its exciton to one of the two down-monomers. Consequently, both monomer and excimer decays are sums of three exponentials. In this case, we were able to evaluate all the rate constants involved and recover the a priori known (from ^{1}H NMR) fraction of isolated monomers (0.23).[25]

There are a number of other possible causes for complexity in fluorescence decays of polymers. For example, the occurrence of energy transfer or migration will change the physical meaning of the parameters recovered from the decays, namely the rate constant for excimer formation k_a and its activation energy E_a. Other example is the formation of ground-state dimers, whenever the ground-state interaction between the chromophores is attractive instead of repulsive (theory predicts that this interaction is attractive, ca. 3 kcal mol^{-1} in the case of PMPS[11]). Under these conditions, the decay laws of monomer and excimer still obey Birks kinetics (sums of two exponentials) but the preexponential factors are affected, as in the case of 1,3-diphenyltetramethyldisiloxane (PMPS2).[20]

Molecular dynamics (MD) can be of help in viewing the configurations of the chain and the kind of rotational transitions that can be responsible for the approach of monomers to excimer forming conformations. MD trajectories give conformational properties as a function of time and, hence, can discriminate between faster and slower transitions. According to MD trajectories (ground state), the mechanism of bond rotation in a siloxane dyad involves coordination between the two skeletal bonds (Si−O and O−Si). They rotate in opposite senses, such that, overall, what rotates is the oxygen (around the axis defined by the line between the two silicons).[1] Along the trajectories, there are no clear-cut jumps between defined states. In the siloxanes, the torsional barriers for backbone rotations are very low, and the steric repulsions between lateral groups are diminished (due to longer bond lengths and wider bond angles, as compared with hydrocarbon polymers). The skeletal rotations occur then almost continuously, without transitions between separated rotational isomers.[1] In fact, the classical rotational isomers are not well-defined in siloxanes, and the rotational angle loses usefulness as conformational variable to follow the approach between neighbor phenyl rings which is necessary for an excimer forming conformation.

The interphenyl distance, d_{ph}, itself is the relevant conformational variable. The approach between phenyl groups (as measured by d_{ph}) is accompanied by the almost parallelism between ring planes and between Si−C bonds[24] (due to the planar structure of the phenyl rings and their bulkiness, which leave little chance to the nonparallel arrangements when d_{ph} gets short enough). The evolution of conformational changes leading to excimer forming configurations can then be followed in terms of just this one variable d_{ph}.

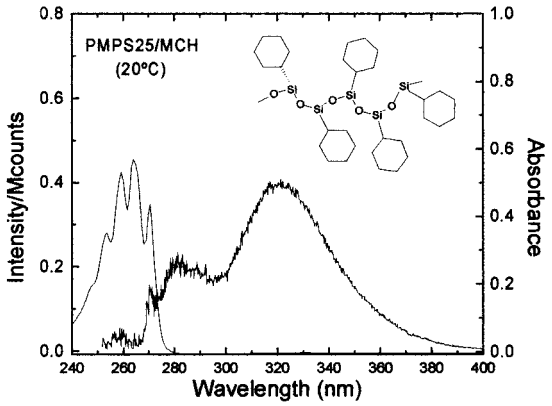

Figure 1. Absorption and fluorescence spectra of PMPS25, in dilute MCH solution, at 20 °C, $\lambda_{ex} = 260$ nm.

In this work, we present the full kinetic analysis of the fluorescence decays of a monodisperse sample of poly(methylphenylsiloxane), PMPS*N*, with an average number of skeletal bonds $N = 25$, measured with picosecond time-resolution. From this analysis, all rate constants and their temperature dependence are evaluated. The resulting dynamic parameters are compared with the results obtained from Molecular dynamics calculations.[1,24]

Experimental Section

Polymer samples, synthesized and characterized by Clarson and Semlyen,[28] were kindly donated by Dr. Semlyen. Samples are named PMPS*N*, *N* being the nominal number-average number of skeletal bonds. Their average molecular weights and polydispersities are given elsewhere.[26] Methylcyclohexane (MCH) from BDH (laboratory reagent) was purified as previously described.[10]

Solutions of PMPS2 and PMPS25 in MCH, with absorbance equal to 0.5 at the excitation wavelength (260 nm) were degassed by the freeze−pump−thaw technique (six cycles at 5×10^{-5} Torr) and then sealed. Under these conditions, polymer concentrations are below the critical value for coil overlap, which makes unlikely intermolecular chain contacts in homogeneous solutions. Solutions of the monomeric model compound (MS) were prepared with exactly the same absorbance at the excitation wavelength. The proper monomeric model compound for PMPS25 is methyldimethoxyphenylsilane.[29]

Ultraviolet absorption and fluorescence spectra were recorded on an Olis-15 spectrophotometer and a Spex Fluorolog F212I fluorimeter, respectively.

Fluorescence decays of the same solutions employed in steady-state measurements, were measured, as a function of temperature, by the time correlated single photon counting technique (SPC), as described before.[10,30] A Millennia X (Spectra Physics, Inc.) plus a frequency-tripled Ti:sapphire picosecond laser system (Spectra Physics, Inc.) was the excitation source ($\lambda_{ex} = 260$ nm, repetition rate 4 MHz, fwhm = 28 ps). Alternate collection of pulse and sample was performed (10^3 counts at the maximum per cycle) until 5×10^3 counts at the maximum were acquired. The fluorescence decays were deconvoluted in a Micro Vax 3100, using an updated version of George Striker's program[31] which allows for single and global analysis and automatic shift correction.

Results

Fluorescence Measurements. Figure 1 shows the absorption and emission spectra of PMPS25 in dilute MCH solution at room

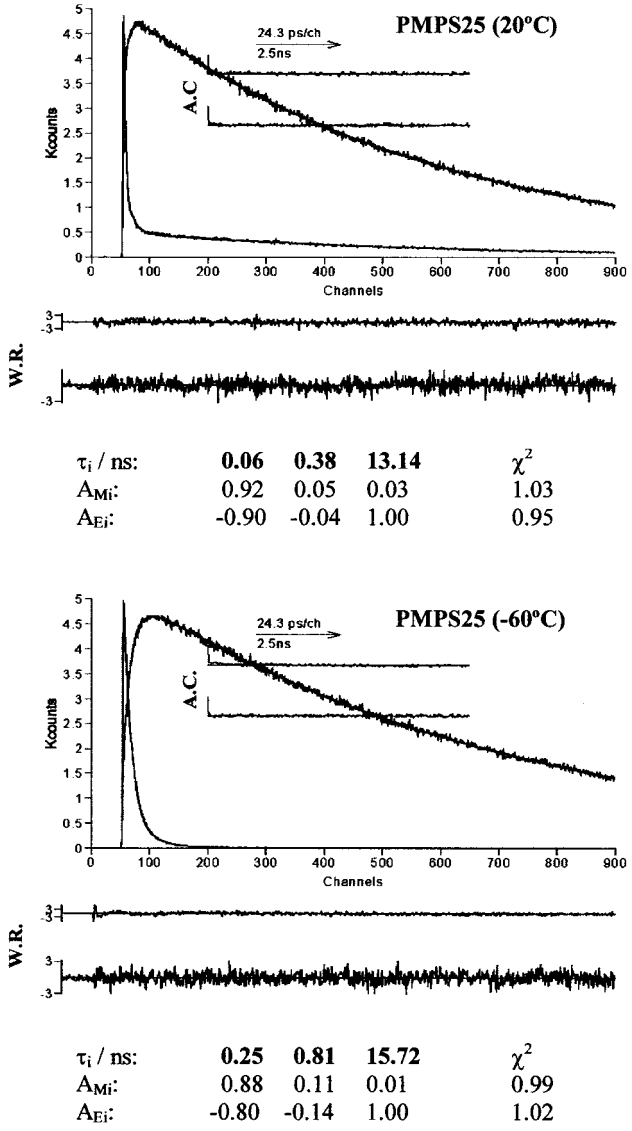

Figure 2. Global analysis of monomer (λ_{em} = 275 nm) and excimer (λ_{em} = 330 nm) decays of PMPS25, in MCH, at 20 °C. Decay times, amplitudes, weighted residuals, and autocorrelation functions are also shown.

temperature (20 °C). Monomer and excimer emission bands centered at about 280 and 320 nm can be observed.

The fluorescence decays of this sample were measured at 275 and 330 nm, as a function of temperature (193−293 K). Figure 2 shows fluorescence decays of PMPS25 at 20 °C and −60 °C. Global analysis of monomer and excimer decays with sums of three exponentials give perfect fits for all temperatures. The independent analysis of monomer and excimer decays of PMPS25, also shows that sums of three exponentials are needed to fit the decays, unlike the dyad model molecule (PMPS2), for which only two are needed.[20,25] The three decay times (τ_I) are similar in the monomer and excimer, meaning that at least three kinetically different species exist in the excited state, as in the case of the cyclic trimer (CMPS3).[25] The same observation has been made for all PMPS*N* samples so far studied by us (*N* = 25, 82, 176, 284, 443, and 1285).[15,16,26]

MEM (maximum entropy method) analysis of monomer decays of PMPS2, CMPS3 and PMPS25 are shown in Figure 3. The three distributions of decay times obtained for the two last samples indicate that ,indeed, three exponentials are sufficient to describe the fluorescence decays of CMPS3 and PMPS25, in the range of temperatures here considered.

The three decay times (τ_i) of PMPS25 and their amplitudes in the monomer (A_{Mi}) and excimer (A_{Ei}) decays, at 20 °C, are given in Table 1. Data obtained for the dyad model (PMPS2) and the cyclic trimer (CMPS3)[25] are included for comparison. Figure 4 shows the temperature dependence of the decay parameters (reciprocal decay times, λ_i, and amplitudes, A_{Mi} and A_{Ei}) obtained with PMPS25.

Two of the three decay times of PMPS25, the shortest (τ_3) and the longest (τ_1) ones, are similar to the two decay times found for PMPS2 and CMPS3 at 20 °C (see Table 1), and show a Birks-like temperature dependence (Figure 4). The major differences reside in the intermediate exponential term, which is nonexistent in the case of PMPS2. When compared to CMPS3, the intermediate decay time (τ_2) in the decay of PMPS25 is much shorter at room temperature, but increases and approaches that of CMPS3 on lowering the temperature. The preexponential factor (A_{M2}) is much lower in the case of PMPS25 than in that of CMPS3 in the whole temperature range, meaning that the intermediate time is much less important in the case of PMPS25 than in the cyclic trimer.

Fluorescence intensities of monomer, excimer and the parent model compound were also measured as a function of temperature, under steady-state conditions. The data are shown in Figure 5 under the form of Stevens−Ban plots.[20]

Molecular Dynamics. The fluorescence decays show that in the excited state of the polymer PMPS25 there is a slow process which is not present in the dyad (the dimer, PMPS2). We used molecular dynamics (MD) to analyze both types of molecules and see what differences can be detected in their respective time behavior. As a model for the PMPS25 chain, we used a polymer fragment called P14. It was constructed with 14 monomer units (28 skeletal bonds) in an heterotactic configuration (same chain length and fraction of meso dyads (0.5) as the actual polymer). The MD calculations have been performed with module Discover 3 from Molecular Simulations, Inc. (San Diego, CA). The force field was the same as described before when reporting conformational energy maps.[11] The temperature for MD was 300 K (the Si−O backbone being very flexible, enough transitions occur at this temparature). This minimized structure is heated gradually until the working temperature is attained. Then, a long thermalization takes place, first by direct velocity scaling for 1 ns, and then with the Nosé method for another 1 ns. After this thermalization, the trajectory in which data are collected starts. The same Nosé method is used, with an integration time-step of 0.25 fs. The frequency of occurrence of conformational states in the MD trajectory reflects true statistical probabilities at *T*, as has been checked thoroughly with the disiloxan model molecule (PMPS2).[24]

Figure 6 shows the time evolution of the interphenyl distance, d_{ph}, for PMPS2 and P14 (d_{ph} as measured between the centers of the phenyl rings). In PMPS2, it is shown the only interphenyl distance of the molecule (Figure 6a). In P14, there are two distances shown (Figure 6b,c), the ones separating one defined phenyl ring (7) to each of its two nearest neighbors in the chain (6 and 8). The phenyl ring chosen occupies an inner position in the 14 monomer units sequence, thus avoiding end effects. Figure 6d is the superposition of Figure 6b,c. Comparing PMPS2 with P14 we can easily detect a difference in the visual appearance between the two types of molecules.

In PMPS2, there is no clear preference for the long or the short distance ranges. Also, in PMPS2, jumps from the long to the short distance ranges occur fairly regularly, at similar intervals. In P14, on the other hand, these jumps occur irregularly along the time. In P14, the interval between

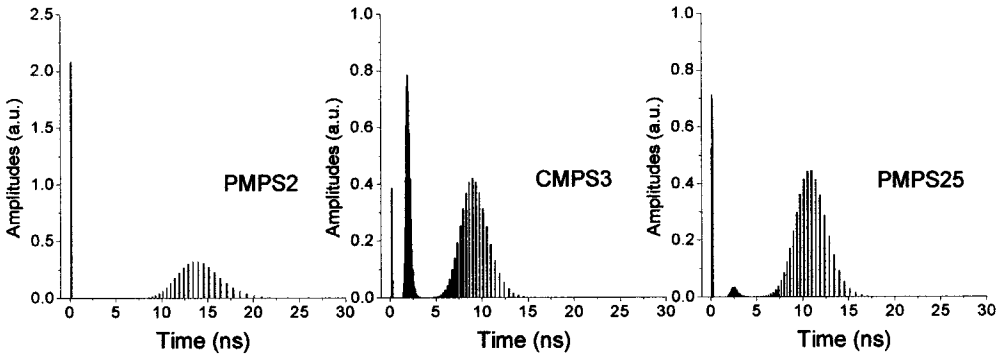

Figure 3. MEM (maximum entropy method) analysis of monomer decays of PMPS2, CMPS3, and PMPS25, in MCH, at 20 °C.

TABLE 1: Summary of Taus and Amplitudes of PMPS2, CMPS3, and PMPS25 in MCH at 20 °C

compound	amplitude	τ_3 (ns)	τ_2 (ns)	τ_1 (ns)	χ^2
PMPS2		0.11		10.75	
	A_{Mi}	0.92		0.08	0.97
	A_{Ei}	−0.71		1.00	1.03
CMPS3		0.06	1.92	9.50	
	A_{Mi}	0.66	0.20	0.14	0.98
	A_{Ei}	−0.83	−0.09	1.00	1.00
PMPS25		0.06	0.38	13.14	
	A_{Mi}	0.92	0.05	0.03	1.03
	A_{Ei}	−0.90	−0.04	1.00	0.95

consecutive jumps is sometimes as short as in PMPS2, but other times is much longer. In these cases, the phenyl ring remains separated from its two neighbors over a long time. In P14 the d_{ph} vs time plot shows ample intervals or "windows" where the phenyl ring remains well separated (isolated) from its two neighbors. The transition of this phenyl ring to an excimer-forming configuration remains frozen for a long period. This is not seen in the trajectory of PMPS2, where the jumps occur more or less uniformly, without such wide windows.

In brief, the transition of a phenyl ring to an excimer forming configuration can get frozen and the chromophore can stay isolated from its neighbors for long periods, when the phenyl ring belongs to a polymer chain. This isolated phenyl ring has its configuration frozen from the point of view of its distance to the neighboring phenyls (Figure 6d), but not from the point of view of the rotation of the skeletal bonds to which the ring is attached. The skeletal bonds continue to rotate during the period of isolation of the lateral group (in the same way that they rotate in any other piece of the trajectory).[1] The permanence of a given interphenyl distance is possible thanks to the almost synchronized rotation of the Si−O and O−Si bonds in the dyad. These two bonds rotate in opposite senses, thus keeping almost the same distance between the two lateral groups of the dyad.[1]

A window opened in the trajectory of the polymer can remain open for a very long period of time (some extend over a very long piece of the trajectory, Figures 6b,d), but the overall weight of the phenyl rings which get isolated is small, because the number of times these windows appear is low (compared to the total number of transitions) and there are two neighbors (Figure 6d).

Figure 7 shows the autocorrelation function of the distance between the centers of phenyl rings. In PMPS2, it is the distance of the only dyad present and, in P14 it is the mean of the autocorrelation functions for the distance of monomer 7 to its two neighbors (6, 8); namely, it is the mean of the distances in dyads 6−7 and 7−8, shown in Figure 6.

First, note that the correlation persists over longer times in the polymer than in the dimer. Second, the autocorrelation function decay in P14 shows two time regimes, while in PMPS2 there is only one. The relaxation times are ca. 6 and 75 ps for P14 and ca. 3.5 ps for PMPS2.

The distribution of transition times has been calculated. It shows that, in P14, only nine out of 10 transitions suffered by a dyad occur within the time interval in which all the transitions of PMPS2 occur. The remaining one requires times much longer than the complete time interval of PMPS2 (about an order of magnitude longer). In these longer periods, we can say that the phenyl rings remain isolated or hindered (without transition). Therefore, this small fraction of hindered units suffers a process that is about 1 order of magnitude slower than the process of PMPS2 and of the remaining units of the polymer.

Discussion

Mechanism. Let us consider first the physical meaning of the intermediate exponential term. Inspection of Figure 4 shows the following: (1) A_{M2} (the amplitude of the intermediate term in the monomer decay) is larger at low temperatures where the excimer dissociation is frozen (i.e., when A_{M1} tends to zero); (2) it loses importance in the excimer decay at low temperatures (A_{E2} decreases on lowering temperature; (3) A_{E2} is negative, that is, τ_2 is a rise-time in the excimer decay. Therefore, the intermediate exponential term must represent a monomer. In addition, A_{M3}/A_{M2} is large, so it represents a minor fraction of monomers and these monomers decay much slower than the majority.

On the basis of the results from MD calculations, these monomers are assigned to isolated hindered monomers M_h, which are kinetically coupled to nonhindered monomers M_{nh}, and excimer E, through the mechanism shown in Scheme 1. M_{nh} and M_h represent monomers in configurations such that their ability to reach an excimeric conformation is controlled, respectively by (a) the local motion of the dyad ("fast" monomers) and (b) the slower rearrangement of longer chain segments ("slow" monomers). M_h* are excited phenyl groups which remain well isolated, that is, separated from their nearest neighbors over long time lapses (much longer than in an independent dyad), which can decay to the ground state (k_M), unblock to a M_{nh}* configuration (k_u) or transfer the excitation to any of the two adjacent phenyl groups (k_t). The nonhindered phenyl groups (M_{nh}*), can form excimers (k_a), decay to the ground state (k_M), transfer energy to an adjacent M_h* (k_t), or become itself an isolated hindered monomer (due to rotations in the rest of the chain) (k_b). The excimer E* can dissociate back to M_{nh}* (k_d) or decay to ground-state monomers (k_E). The model also takes into account the possibility of excimer formation by direct absorption of light of α ground-state monomer units forming ground-state dimers M_0. The molar fraction of hindered ground-state monomers M_h is represented by β and I_o is the rate of light absorption by all monomers, at the excitation wavelength.

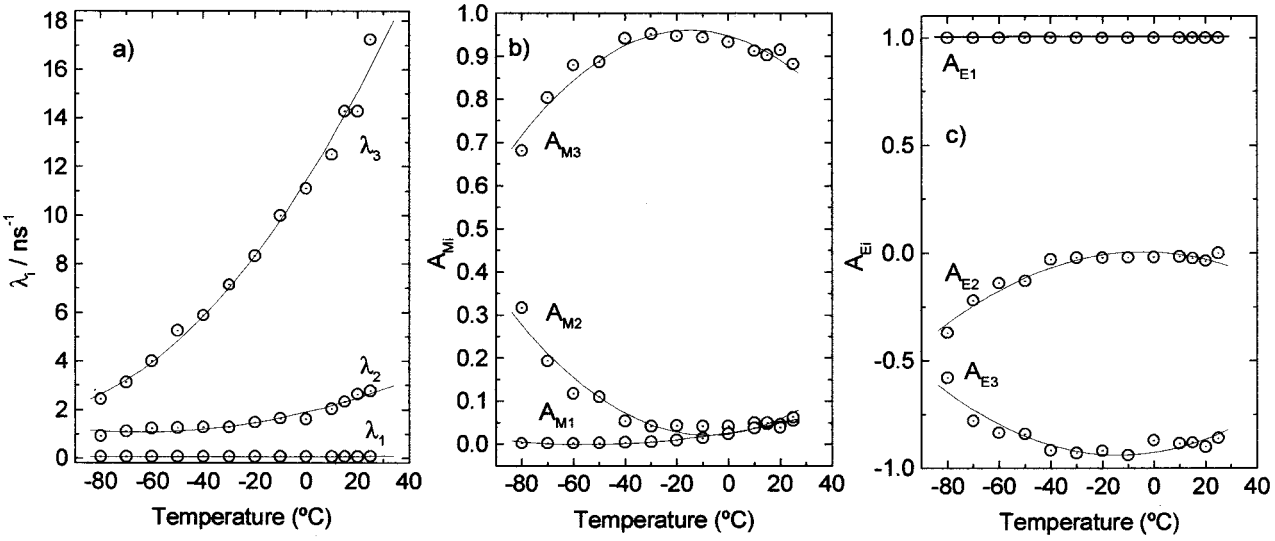

Figure 4. Temperature dependence of the three reciprocal decay times (λ_1, λ_2, and λ_3) and the preexponential factors at the monomer (A_{M1}, A_{M2}, and A_{M3}) and at the excimer (A_{E1}, A_{E2}, and A_{E3}) emission wavelengths of PMPS25, in MCH, at 20 °C: (○) experimental data, (—) calculated with (A2) through (A7).

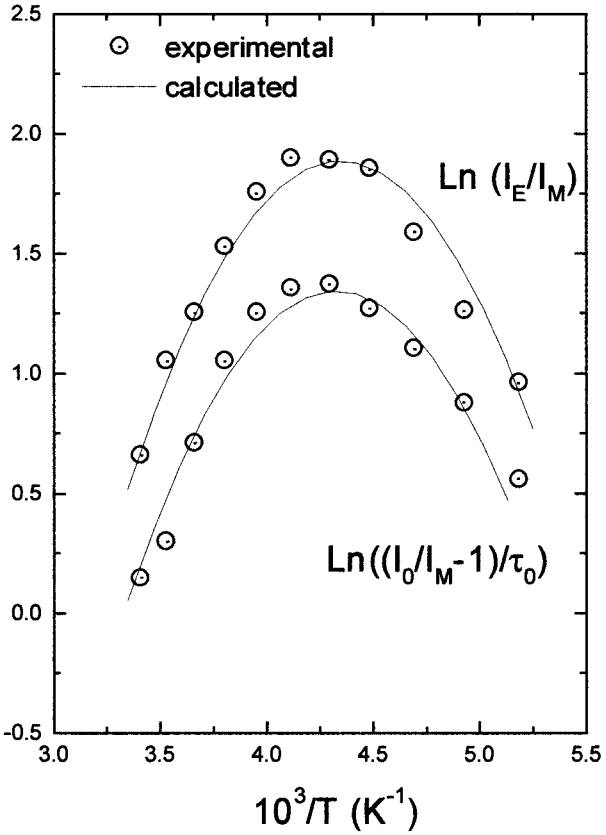

Figure 5. Stevans−Ban plots of PMPS25 in MCH: (○) steady-state experimental data, (—) calculated with time-resolved data in (A8) and (A9).

The rate constant k_1 in Scheme 1 is the sum of the unblocking (k_u) and the energy transfer rate constants. The value of the last one is the product of the energy transfer rate constant to one neighboring phenyl unit (k_t) multiplied by the probability that this is an nonhindered monomer ($1 - \beta$), multiplied by 2 (because there are two neighbors),

$$k_1 = k_u + 2(1 - \beta)k_t \tag{1}$$

The rate constant for the inverse process k_2 has a similar form,

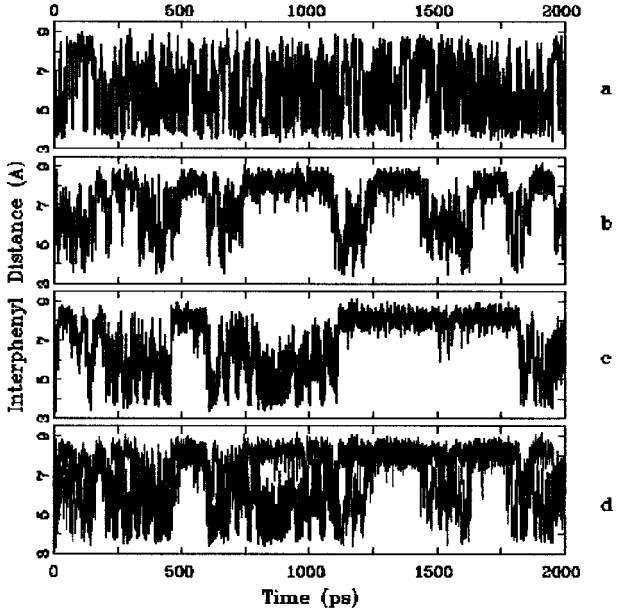

Figure 6. Interphenyl (center-to-center) distance (d_{ph}) as a function of time, along a molecular dynamics trajectory: (a) the dyad in PMPS2, (b) the dyad 6−7 in P14, (c) the dyad 7−8 in P14, and (d) superposition of dyads 6−7 and 7−8.

except that k_t is now multiplied by the probability that the neighboring phenyl is a "slow monomer" (β):

$$k_2 = k_b + 2\beta k_t \tag{2}$$

The rate constants k_u and k_b are connected by the equilibrium condition:

$$\frac{k_u}{k_b} = \frac{1 - \beta}{\beta} \tag{3}$$

Substitution of (3) in (2) leads to the relation $k_2 = k_1(\beta/(1 - \beta))$ or, if we write $\beta' = \beta/(1 - \beta)$, to

$$k_2 = \beta' k_1 \tag{4}$$

Kinetics. Equation 5 rules the time evolution of the concentrations vector of the three species in Scheme 1.

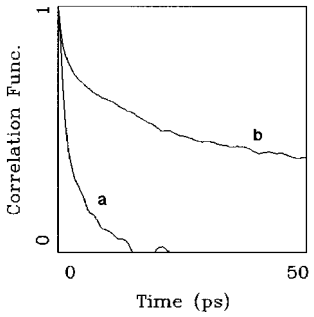

Figure 7. Autocorrelation functions for the distance between centers of the phenyl rings (d_{ph}): (a) PMPS2 and (b) P14 (it is the mean of the autocorrelation functions for the distance of monomer 7 to its two neighbors (6, 8); namely, it is the mean of the distances in dyads 6−7 and 7−8).

SCHEME 1

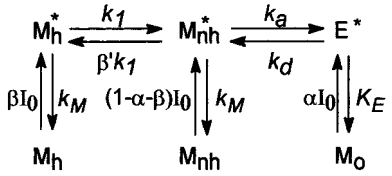

$$\frac{d}{dt}\begin{bmatrix} M_h^* \\ M_{nh}^* \\ E^* \end{bmatrix} = \begin{bmatrix} -(k_1 + k_M) & \beta' k_1 & 0 \\ k_1 & -(\beta' k_1 + k_M + k_a) & k_d \\ 0 & k_a & -(k_E + k_d) \end{bmatrix} \times \begin{bmatrix} M_h^* \\ M_{nh}^* \\ E^* \end{bmatrix} \quad (5)$$

Integration of (5) leads to (see Appendix):

$$\begin{bmatrix} M_h^* \\ M_{nh}^* \\ E^* \end{bmatrix} = \begin{bmatrix} a_{11} & a_{12} & a_{13} \\ a_{21} & a_{22} & a_{23} \\ a_{31} & a_{22} & a_{33} \end{bmatrix} \times \begin{bmatrix} e^{-\lambda_1 t} \\ e^{-\lambda_2 t} \\ e^{-\lambda_3 t} \end{bmatrix} \quad (6)$$

where λ_1, λ_2, and λ_3 are reciprocal decay times and the a_{ij} ($i,j = 1$, 2, and 3) are preexponential coefficients.

The reciprocal decay times (λ_j) are the roots of the characteristic equation of the transformation matrix:

$$\lambda^3 - \lambda^2(\beta' k_1 + k_M + k_a + X + Y) + \lambda[(X + Y)(\beta' k_1 + k_M + k_a) + XY - k_a k_d - \beta' k_1^2] + X k_a k_d + Y\beta' k_1^2 - XY(\beta' k_1 + k_M + k_a) = 0 \quad (7)$$

where $X = k_1 + k_M$ and $Y = k_E + k_d$.

Expressions for the preexponential coefficients (a_{ij}) are also given in the Appendix.

Data Analysis. The experimental fluorescence intensity (collected at the monomer emission wavelength) is the sum of emissions of M_h and M_{nh} monomers,

$$I_M(t) = I_{M_h}(t) + I_{M_{nh}}(t) = \sum_{j=1}^{3} A_{Mj} \exp(-\lambda_j t) \quad (8)$$

and the excimer emission intensity is given by (9).

$$I_E(t) = \sum_{j=1}^{3} A_{E_j} \exp(-\lambda_j t) \quad (9)$$

The experimental amplitudes A_{Mj} and A_{Ej} are related to the preexponential coefficients by

$$A_{Mj} = k_{f_M} \times f_M \times (a_{1j} + a_{2j}) \qquad (j = 1, 2, 3) \quad (10)$$

$$A_{Ej} = k_{f_E} \times f_E \times a_{3j} \qquad (j = 1, 2, 3) \quad (11)$$

where k_{fM} and k_{fE} are the monomer and excimer radiative rate constants and f_M and f_E are instrumental factors.

In Scheme 1 there are seven unknowns (k_1, k_a, k_d, k_E, k_M, α, and β) and the available experimental parameters are eight: λ_1, λ_2, λ_3, A_{M3}/A_{M2}, A_{M3}/A_{M1}, A_{E3}/A_{E2}, A_{E3}/A_{E1}, and k_M (measured with the monomeric model compound). The numerical evaluation of the unknowns was done using the "fmins" routine (AT-MATLAB package) to minimize the residuals of the seven following relations, at each temperature (see also Appendix):

$$\sum_{i=1}^{3} \lambda_i - (\beta' k_1 + k_a + k_M + X + Y) = 0 \quad (12)$$

$$\sum_{\substack{i,j=1 \\ j>1}}^{3} \lambda_i \lambda_j - (Y(\beta' k_1 + k_a + k_M) + X(Y + \beta' k_1 + k_a + k_M) - k_a k_d - \beta' k_1^2) = 0 \quad (13)$$

$$\lambda_1 \lambda_2 \lambda_3 - (XY(\beta' k_1 + k_a + k_M) - X k_a k_d - \beta' k_1^2 Y) = 0 \quad (14)$$

$$\frac{A_{M3}}{A_{M2}} - \left(\frac{a_{13} + a_{23}}{a_{12} + a_{22}}\right) = 0 \quad (15)$$

$$\frac{A_{M3}}{A_{M1}} - \left(\frac{a_{13} + a_{23}}{a_{11} + a_{21}}\right) = 0 \quad (16)$$

$$\frac{A_{E3}}{A_{E2}} - \left(\frac{a_{33}}{a_{32}}\right) = 0 \quad (17)$$

$$\frac{A_{E3}}{A_{E1}} - \left(\frac{a_{33}}{a_{31}}\right) = 0 \quad (18)$$

In all cases convergence was attained independently from the initial guess of parameters. The results are shown in Figure 8.

The Arrhenius plots are linear for all rate constants except for k_1, where the upward curvature in the high-temperature region, suggests the contribution of both an activated and a nonactivated process as predicted by (1) (in the case of CMPS3, k_1 is temperature independent[25]). The fact that both the activated (k_u controlled) and the nonactivated (k_t controlled) regions are contained in the covered temperature range, allows the splitting of these two contributions. Thus, k_1 was fitted with (1) under the assumptions that k_t is temperature independent and k_u obeys an Arrhenius type temperature dependence. The results from the analysis of the data shown in Figure 8 are given in Table 2.

Self-consistency of these results was evaluated in three ways. First, the data in Table 2 was used in (A2−A7) to simulate the time-resolved experimental parameters: reciprocal decay times (λ_j), and experimental amplitudes (A_{Mj} and A_{Ej}). Simulated curves are plotted with experimental data in Figure 4.

Second, the same data was used in (A8 and A9) to simulate the experimental I_0/I and I_E/I steady-state results (lines in Figure 5).

Third, the d_{ph} (distance between the centers of phenyl rings) probability density function $f(r)$, obtained from MD results for

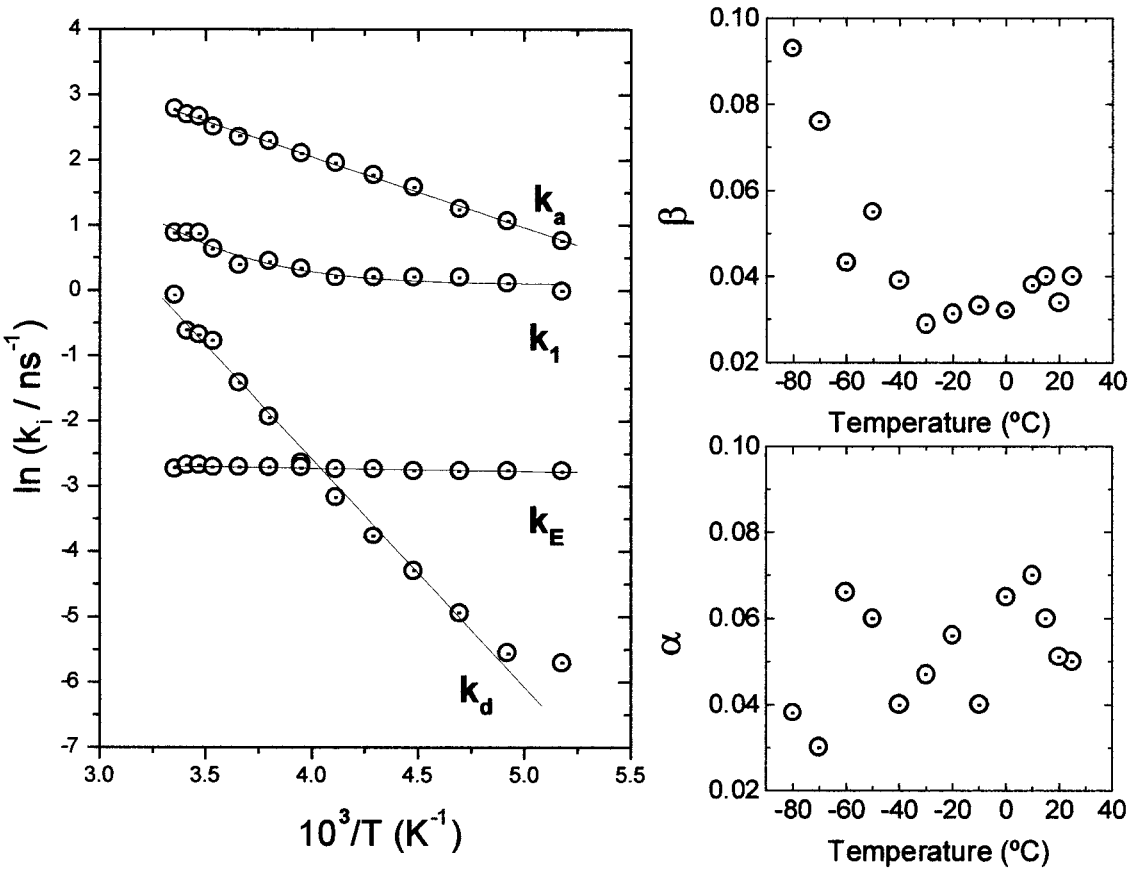

Figure 8. Arrhenius type plots of the rate constants k_I obtained for PMPS25 from the kinetic analysis of time-resolved results measurements.

TABLE 2: Values of Rate Constants, Activation Energies, and Fractions of Hindered Monomers (β) and Preformed Dimers (α) Obtained for PMPS2, CMPS3, and PMPS25, in MCH Solution, from Time-Resolved Results

	PMPS2	CMPS3[a]	PMPS25
k_a, 20 °C/10^9 s^{-1}	8.4 ± 0.4	13.7 ± 0.5	14.2 ± 0.5
k_d, 20 °C/10^9 s^{-1}	0.66 ± 0.06	1.64 ± 0.4	0.58 ± 0.1
k_u, 20 °C/10^9 s^{-1}			1.21 ± 0.2
k_t/10^9 s^{-1}		0.13 ± 0.01	0.56 ± 0.1
k_M, 20 °C/10^9 s^{-1}	0.267 ± 0.003	0.267 ± 0.003	0.267 ± 0.003
k_E, 20 °C/10^9 s^{-1}	0.074 ± 0.006	0.070 ± 0.006	0.068 ± 0.006
E_a/kcal mol^{-1}	2.5 ± 0.1	2.2 ± 0.2	2.2 ± 0.2
E_d/kcal mol^{-1}	7.4 ± 0.2	6.6 ± 0.3	6.9 ± 0.3
E_u/kcal mol^{-1}			5.6 ± 1.3
α	0	0.04 ± 0.015	0.05 ± 0.02
β	-	0.23 ± 0.02	0.04 ± 0.02

[a] Data from ref 25.

CMPS3 and PMPS25,[24] was used to calculate the rate constant for energy transfer through the Förster mechanism (19):[32]

$$k_{ET} = k_M R_0^6 \int f(r)\left(\frac{1}{r}\right)^6 dr \qquad (19)$$

The critical distance for energy transfer, $R_0 = 7.25$ Å, was determined with the monomeric model compound (dimethoxymethylphenylsilane).[29] The calculated values of the energy transfer rate constants, $k_{ET}=0.14 \times 10^9$ s^{-1} for CMPS3 and $k_{ET}=0.39 \times 10^9$ s^{-1} for PMPS25, are in agreement with the experimental observation that k_t has a significantly larger value for PMPS25.

There are other relevant observations to be made in Table 2. First, the rate constant of the fast excimer formation process k_a has similar values for CMPS3 and PMPS25, and these are about twice the value found for PMPS2 (Table 2). Part of the explanation is that in PMPS2 each phenyl has only one neighbor, while in the PMPS25 each phenyl has two. In CMPS3, although 75% of phenyls have just one neighbor,[25] the average distances between them is shorter than in PMPS2 or PMPS25.[24] The short component in the decays of CMPS3 is the average decay of phenyls with both one and two neighbors, because these are too similar and short to be experimentally resolved.

Second, the activation energy E_a is lower or similar to the activation energy for viscous flow in MCH (2.4 kcal mol^{-1}), which denotes a negligible contribution of chain activation barriers for this process.

Third, the slow process of excimer formation seems to have a substantial energy barrier E_u, comparable to the excimer dissociation activation energy E_d.

Fourth, energy migration is excluded on the basis of $(1-\beta)$ being near unity, i.e., the probability of energy transfer to a nonhindered monomer, M_{nh}, is approximately one. For this last one, the rate constant of excimer formation is 50 times larger than the energy transfer rate constant, which means that the probability of a second energy transfer step is about 0.02.

Finally, preformed dimers can be ignored in PMPS25 (α = 0.05), as found with CMPS3.[25]

Molecular Dynamics. The transitions to an excimer forming configuration (jumps from the long distance range to the short distance range) suffer a delay in the polymer chain. It is thus caused by the attachment of the dyad to a polymer backbone. The delay can be very long, so some units are really retarded in their transition rate. But these long delays appear only a few times along the trajectory, so the fraction of units involved in this retardation is small. All these characteristics are in accordance to what the kinetic scheme attributes to the isolated monomers. Therefore, simulation results lend support for the kinetic analysis.

The reason for this delay in linear chains must be due to the

hindrance imposed by the long pieces of chain attached to the ends of the rotating bonds. In the case of PMPS2, the only requisite is that the pair of bonds rotate in a coordinated fashion. But, for longer sequences, the rotations have to be accommodated along the chain, so that no large sweeping of space occurs.

The problem of how the rotational transitions which take place in the middle of a polymer chain are accommodated or localized by local motions in the topological neighbors is the subject of much interest.[33,34] Models and atomistic simulations are being used to analyze the mechanisms which contribute to such localization. Cooperative transitions which occur in pairs (the early proposal in models) are not the general rule.[34−38] Atomistic calculations of C−C and C−O polymers show that many transitions occur isolated.[34−38] Coupled small amplitude rearrangements of the adjacent torsions can localize the motion without a second conformational transition. It has been found that conformational transitions are localized within 8−10 atoms along the polymer chain.[34−38] In these studies, the conformational transitions which have to be localized are discrete jumps between two rotameric states.

Here, we have a different problem. In the siloxane chain the rotameric states and the rotational transitions are not sharply defined. Besides, the rotations of the two bonds in a dyad are strongly coupled. But these coupled rotations do not necessarily lead to the transition of interest here. The transition is between two interphenyl distance states, not between two rotameric states. We have two time scales, a short one, which corresponds to bond rotations, and a long one, which corresponds to the jumps from the separated to the close interphenyl distance states. This long time scale is the one that should be related to experimental decays involving excimer formation.

In this long time scale, we still have two regimes. One for the small molecules, in which the residence times for the separated and the close distance states are similar. Another for the polymer chain, in which a much longer residence time appears for the separated distance state. The problem here is to explain how the topological neighbors of a dyad freeze this transition, maintaining the separated distance state for such long times. Probably, there is a connection with the mechanism by which conformational transitions associated with a rotameric jump are localized.

The position of the dyad along the chain has influence on this long time. The "windows" we see in Figure 6 are for the middle dyads. The "windows" for the dyads placed at the end of the chain fragment are shorter. Thus, the mechanism by which the distance state remains frozen is more effective when both sides of the dyad have long tails attached to it. This is similar to what has been found in a polystyrene fragment (but referred to a different property).[39] The mean relaxation time for the decay of the orientational correlation function (for the vector between two consecutive substituted C atoms, equivalent to a dyad) is larger for the dyads in the middle of the fragment (in good accord with experimental results of fluorescence depolarization).[39,40]

The long time scale (where the transitions between interphenyl distance states occur) can be considered as the superposition of two processes, in the case of the polymer chain. One is the jump from the separated to the close distance state. The other is the delay that freezes this transition over long times. We can call a transition that occurs without delay as "fast" and a transition that occurs after delay as "slow". Fast transitions occur in all molecules (small and polymer). In fact, are the only ones that occur in the small dimer. For this fast process the only requisite is the coordinated two bond rotation of the dyad. Slow transitions only occur in the polymer. The longer sequence accommodation, which needs correlation with other dyads, is likely what makes a particular phenyl ring to stay frozen for long pieces of the trajectory.

Let us consider now our results for cyclic trimer (CMPS3). Experimentally there is also a third decay component, which was shown to come from the trans phenyl of the isomer trans.[25] The MD trajectories for the two isomers of CMPS3 show that the time evolution of the interphenyl distances is like that in PMPS2. The distribution of transition times is narrow with values in the same range as found for PMPS2.[24] So, the process in the cyclic trimer is only of the "fast" type. There are no "slow" monomers. The phenyl ring in trans never gives the transition.

Fast and Slow Motions in PMPS. Several interpretations can be proposed to harmonize photophysical and MD results, by ascription of the fast and slow motions observed in fluorescence decays to motions and transitions observed in MD. It may be hypothesized that:

1. The slow motion corresponds to the approach of the two rings whereas the fast one is only a local rearrangement to make them perfect parallel. The fast motion would thus be governed by excited state potential interactions between rings, and would be only slightly dependent on solvent viscosity and temperature. The activation energy of k_a, the rate constant for the fast motion, is not too large (see Table 2), but it is larger than expected for such a rearrangement. Nevertheless, this assignment of the fast motion must be discarded because the fast motion is the only dynamic mechanism for excimer formation in CMPS3, and through MD it is clearly observed that in this strained cycle, restricted rotations of only ±40° are responsible for the approach of rings to the excimer configuration.

2. The fast motion corresponds to approaching of two nearest neighbor rings (N and $N+1$) and the slower one to approaching of ring N with $N+2$ and $N+3$. Such nonnearest neighbor contacts were demonstrated by MD,[24] although they represent only about 2−3% of contacts between nearest neighbors (N and $N+1$). These slow motions are segmental non Arrhenius diffusion better than Arrhenius rotation-like motions and the apparent activation energy should be slightly larger than 2.4 kcal/mol, the activation energy for viscous flow in MCH. Both k_u and E_u were determined with some uncertainty, but it can be concluded that they do not follow such conditions and, therefore, this ascription may also be discarded. Furthermore, excimers not kinetically coupled, such as these, would imply two different types of excimers, something that is not observed in decays. The decays prove the existence of two types of monomers and only one excimer.

3. Slow and fast rotations come from conformations with different energetic barriers. The reason for that difference could be, in principle, similar to that of RIS of hydrocarbon polymers. But that is not the case for siloxanes. Very low barriers in the siloxanes separate the states, and these barriers are the same in the small PMPS2 and in PMPSN.

4. A source of different energetic barriers may come from different stereochemical configurations. The polymer chain contains dyads that are meso and dyads that are racemic, while PMPS2 has just one configuration. It would be reasonable to think that meso and racemic dyads could have different energetic barriers and thus different rate constants for motions from nonexcimer (long distance) to excimer forming configurations. But again, they would not be monomer species kinetically coupled (Scheme 1), because a meso dyad may not be

transformed in a racemic one. Besides, from the point of view of the tacticity, any monomer is equivalent to the others, both in the simulated chain and (approximately) in real chains, since any monomer belongs to a meso dyad on one side and to a racemic dyad on the other side.

Conclusions

If we discard the four possibilities above in the section "Fast and Slow Motions in PMPS", we can conclude that the right interpretation of our results is the following: The fast motion corresponds to PMPS*N* transitions which are common with PMPS2 and CMPS3, whereas the slow motion is particular of the polymer. Molecular dynamics shows that chain monomers are trapped in the long distance state for long times. The dynamic consequence of that is to decrease the number of transitions to the short distance state, what, in terms of excimer formation, would mean that excimer formation would be slower for such monomers. This trapping of the chain monomers in the long distance state occurs in only about 1 every 10 transitions of a dyad. For the rest it behaves as a monomer in a small molecule, showing fast transitions. This means that monomers showing slower transitions to excimer forming state are coupled with those having fast transitions as considered in Scheme 1. In summary, putting together MD and photophysical results, it can be said that (1) any monomer in linear PMPS*N* may form excimers through a fast motion of approaching neighbor rings, similar in rate and mechanism to that in PMPS2 and CMPS3, and (2) chain monomers in PMPS*N* may also form excimers much slowly, through the same motion than before but after being trapped or isolated during a period of time in the long distance state. As shown in Scheme 1, excimers may also be formed by non dynamic mechanisms, namely, direct absorption of light by rings in excimer forming configuration (short distance states) and by energy transfer from isolated monomers to others in the long distance state but non trapped, able to move to the short distance state.

Can the behavior here observed be common to other polymer systems, or is it peculiar to our case? Siloxane chains are much more flexible than the hydrocarbon structures usually studied. One consequence of this is that excimer formation from M_{nh} (k_a) occurs with a high rate (10^{10} s^{-1} range), much higher than k_1, the rate of interconversion between monomers M_h and M_{nh} (10^9 s^{-1} range). The fast escape of M_{nh} to the excimer is kinetically equivalent to a faster "decay" of M_h (k_M+k_a). The condition that M_h (or M_{nh}) does not "decay" much slower than they interconvert is required to distinguish the two types of monomers. If for instance k_a would be in the 10^7-10^8 s^{-1} range, M_h and M_{nh} would be in the so-called fast equilibrium condition (k_1, $(1-\beta)k_1 \gg k_M$, $k_M + k_a$) and they would appear as one single kinetic species, that is, experimentally undistinguishable in the fluorescence decays.[23]

In molecular dynamics these two processes can be identified also thanks to the existence of numerous transitions within reasonable stretches of the trajectory. Therefore, our contention is that we are in front of a behavior that can be general, and appears here with a sufficient degree of discrimination, because of the flexibility of the structure.

Acknowledgment. Thanks are given to Dr. J. A. Semlyen for generously providing the polymer samples (synthesized and characterized by S. J. Clarson and J. A. Semlyen in Prof. Semlyen's laboratory). Financial supports from ITQB (Portugal), and DGI (Spain), under grants E-45/97 (Portugal) and BQU2000-0251 (Spain), are gratefully acknowledged. Fernando B. Dias aknowledges FCT (Portugal) for the grant PRAXIS XXI/9017/96 and J.C. Lima thanks ITQB for a Post-Doc grant. A.L.M. thanks George Striker for making his deconvolution program available.

Appendix

The solution of (5) is

$$\begin{bmatrix} M_h^* \\ M_{nh} \\ E^* \end{bmatrix} = \begin{bmatrix} a_{11} & a_{12} & a_{13} \\ a_{21} & a_{22} & a_{23} \\ a_{31} & a_{22} & a_{33} \end{bmatrix} \times \begin{bmatrix} e^{-\lambda_1 t} \\ e^{-\lambda_2 t} \\ e^{-\lambda_3 t} \end{bmatrix} \quad \text{(A1)}$$

The λ_1, λ_2, and λ_3 are the *eigenvalues* of the transformation matrix and the a_{ij} ($i,j = 1$, 2, and 3) are the linear combinations of the *eigenvectors* basis set obeying the initial conditions:

$$\sum_{j=1}^{3} a_{1j} = \beta \quad \text{(A2)}$$

$$\sum_{j=1}^{3} a_{2j} = 1 - \alpha - \beta \quad \text{(A3)}$$

$$\sum_{j=1}^{3} a_{3j} = \alpha \quad \text{(A4)}$$

The λ_j are the roots of the characteristic equation of the transformation matrix:

$$\lambda^3 - \lambda^2(\beta' k_1 + k_M + k_a + X + Y) + \lambda[(X+Y)(\beta' k_1 + k_M + k_a) + XY - k_a k_d - \beta' k_1^2] + X k_a k_d + Y\beta' k_1^2 - XY(\beta' k_1 + k_M + k_a) = 0 \quad \text{(A5)}$$

where $X = k_1 + k_M$ and $Y = k_E + k_d$.

The preexponential coefficients (a_{ij}) can be expressed as functions of the kinetic parameters (k_1, k_a, k_d, k_E, k_M, α and β) as follows. Substitution of (A1) in (5) gives

$$\frac{d}{dt}\begin{bmatrix} M_h^* \\ M_{nh}^* \\ E^* \end{bmatrix} = \begin{bmatrix} -(k_1 + k_M) & \beta' k_1 & 0 \\ k_1 & -(\beta' k_1 + k_M + k_a) & k_d \\ 0 & k_a & -(k_E + k_d) \end{bmatrix} \times \begin{bmatrix} a_{11} & a_{12} & a_{13} \\ a_{21} & a_{22} & a_{23} \\ a_{31} & a_{22} & a_{33} \end{bmatrix} \times \begin{bmatrix} e^{-\lambda_1 t} \\ e^{-\lambda_2 t} \\ e^{-\lambda_3 t} \end{bmatrix} \quad \text{(A6)}$$

and the derivation of (A1) yields

$$\frac{d}{dt}\begin{bmatrix} M_h^* \\ M_{nh}^* \\ E^* \end{bmatrix} = \begin{bmatrix} a_{11} & a_{12} & a_{13} \\ a_{21} & a_{22} & a_{23} \\ a_{31} & a_{22} & a_{33} \end{bmatrix} \times \begin{bmatrix} -\lambda_1 & 0 & 0 \\ 0 & -\lambda_2 & 0 \\ 0 & 0 & -\lambda_3 \end{bmatrix} \times \begin{bmatrix} e^{-\lambda_1 t} \\ e^{-\lambda_2 t} \\ e^{-\lambda_3 t} \end{bmatrix} \quad \text{(A7)}$$

From (A6) and (A7) and taking into account the initial conditions (A2), (A3), and (A4), the following relations are obtained:

$$a_{11} = Ma_{21};\ a_{12} = La_{22};\ a_{13} = Ja_{23};$$

$$a_{31} = Ia_{21};\ a_{32} = Ha_{22};\ a_{33} = Ga_{23}$$

$$a_{21} = (1 - \alpha - \beta) - a_{22} - a_{23};$$

$$a_{22} = \frac{FA - DC}{EA - DB};\ a_{23} = \frac{CE - BF}{EA - DB};$$

where

$$A = \frac{k_a}{\lambda_1 - Y} - \frac{k_a}{\lambda_3 - Y};\ B = \frac{k_a}{\lambda_1 - Y} - \frac{k_a}{\lambda_2 - Y};$$

$$C = \alpha + (1 - \alpha - \beta)\frac{k_a}{\lambda_1 - Y}$$

$$D = \frac{\beta' k_1}{\lambda_1 - X} - \frac{\beta' k_1}{\lambda_3 - X};\ E = \frac{\beta' k_1}{\lambda_1 - X} - \frac{\beta' k_1}{\lambda_2 - X};$$

$$F = \beta + (1 - \alpha - \beta)\frac{\beta' k_1}{\lambda_1 - X}$$

$$G = \frac{-k_a}{\lambda_3 - Y};\ H = \frac{-k_a}{\lambda_2 - Y};\ I = \frac{-k_a}{\lambda_1 - Y}$$

$$J = \frac{-\beta' k_1}{\lambda_3 - X};\ L = \frac{-\beta' k_1}{\lambda_2 - X};\ M = \frac{-\beta' k_1}{\lambda_1 - X};$$

The numerical calculation starts with a set of initial parameters, from which a_{22}, a_{23}, and a_{21} are calculated. These in turn are used to the calculation of the remaining preexponential coefficients a_{ij} and preexponential factors A_{ij}.

Under steady-state irradiation conditions, the relationships between the fluorescence intensities of monomer I_M, excimer I_E, and parent compound I_0 are given by the following equations:

$$\frac{I_E}{I_M} = \frac{k_{f_E}}{k_{f_M}} \frac{\alpha k_M(\beta' k_1 + k_1 + k_M) + k_a(k_1 + (1 - \beta)k_M)}{(k_d + (1 - \alpha)k_E)(\beta' k_1 + k_1 + k_M) + \beta k_E} \quad \text{(A8)}$$

$$\left(\frac{I_0}{I_M} - 1\right)k_M = \frac{\alpha k_M(\beta' k_1 + k_1 + k_M) + k_a(k_1 + (1 - \beta)k_M)}{(k_d + (1 - \alpha)k_E)(\beta' k_1 + k_1 + k_M) + \beta k_E k_a} k_E \quad \text{(A9)}$$

References and Notes

(1) Horta, A.; Maçanita, A. L.; Freire, J. J.; Piérola, I. F. *Polym. Int*. **1999**, *48*, 665.

(2) Winnik, M. A. *Photophysical and Photochemical Tools in Polymer Science*; NATO ASI Series, Dordrecht, 1986.

(3) Klöpffer, M. H.; Bokobza, L.; Monnerie, L. *Macromolecules* **1998**, *31*, 8291.

(4) Winnik, M. A.; Bystryak, S. M.; Liu, Z.; Siddiqui, J. *Macromolecules* **1998**, *31*, 6855.

(5) Zhao, H.; Lei, Z.; Huang, B. *Polym. J*. **1998**, *30*, 149.

(6) Conwell, E. *Trends Polym. Sci*. **1997**, *5*, 218.

(7) Martín, O.; Mendicuti, F.; Saiz, E.; Mattice, W. L. *J. Polym. Sci., Polym. Phys. Ed*. **1996**, *34*, 2623.

(8) Semerak, S. N.; Frank, C. W. *Adv. Polym. Sci* **1983**, *54*, 31.

(9) Salom, C.; Semlyen, J. A.; Clarson, S.; Hernández-Fuentes, I.; Maçanita, A.; Horta, A.; Piérola, I. F. *Macromolecules* **1991**, *24*, 6827.

(10) Maçanita, A. L.; Piérola, I. F.; Horta, A. *Macromolecules* **1991**, *24*, 1293.

(11) Freire, J. J.; Piérola, I. F.; Horta, I. F. *Macromolecules* **1996**, *29*, 5143.

(12) Horta, A.; Piérola, I. F.; Rubio, A.; Freire, J. J. *Macromolecules* **1991**, *24*, 3121.

(13) Rubio, A.; Freire, J. J.; Piérola, I. F.; Horta, A. *Macromolecules* **1989**, *22*, 4014.

(14) Maçanita, A. L.; Horta, A.; Piérola, I. F. *Macromol. Symp*. **1994**, *84*, 365.

(15) Horta, A.; Piérola, I. F.; Maçanita, A. L. In *Polymeric Materials Encyclopedia*; Salamone, J. C., Ed.; CRC Press: Boca Ratón, FL, 1996; Vol. 8, p 6391.

(16) Maçanita, A. L. in *Plenary Lectures III Congreso de Fotoquímica*; Armesto, D., Orellana, G., Piérola, I. F., Eds.; UNED: Madrid, Spain, 1996.

(17) Maçanita, A. L.; Horta, A.; Piérola, I. F. *Macromolecules* **1994**, *27*, 3797.

(18) Hamaminishi, K.; Shizuka, H. *J. Chem. Soc., Faraday Trans*. **1993**, *89*, 3007.

(19) Itoh, T.; Yang, H. M.; Chou, C. *J. Chem. Soc., Faraday Trans*. **1996**, *92*, 3593.

(20) Maçanita, A. L.; Horta, A.; Piérola, I. F. *Macromolecules* **1994**, *27*, 958.

(21) Wu, S. K.; Jiang, Y. C.; Rabek, J. F. *Polym. Bull*. **1980**, *3*, 319.

(22) Itoh, T. *Macromolecules* **1997**, *22*, 66999.

(23) Vigil, M. R.; Renamayor, C. S.; Piérola, I. F.; Lima, J. C.; Melo, E. C.; Maçanita, A. L. *Chem. Phys. Lett*. **1998**, *287*, 379.

(24) Horta, A.; Piérola, I. F.; Maçanita, A. L. *Macromolecules* **2000**, *33*, 1213.

(25) Dias, F. B.; Lima, J. C.; Maçanita, A. L.; Horta, A.; Piérola, I. F. *J. Phys. Chem. A* **2000**, *104*, 17.

(26) Dias, F. B.; Lima, J. C.; Maçanita, A. L.; Clarson, S. J.; Horta, A.; Piérola, I. F. *Macromolecules* **2000**, *33*, 4772.

(27) De Schryver, F. C.; Collart, P.; Vandendriessche, J.; Goedeweeck, R.; Swinnen, A.; Van der Auweraer, *Acc. Chem. Res*. **1987**, *20*, 159.

(28) Clarson, S. J.; Semlyen, J. A. *Polymer* **1986**, *27*, 1633.

(29) Maçanita, A. L.; Danesh, P.; Peral, F.; Horta, A.; Piérola, I. F. *J. Phys. Chem*. **1994**, *98*, 6548.

(30) Maçanita, A. L.; Costa, F. P.; Costa, S. M. B.; Melo, E. C.; Santos, H. *J. Phys. Chem*. **1989**, *93*, 336.

(31) Striker, G. In *Deconvolution and Reconvolution of Analytical Signals*; Bouchy, M., Ed.; DPIC, Nancy, 1982.

(32) Förster, Th. *Discuss. Faraday Soc*. **1959**, *277*, 7.

(33) Bahar, I.; Erman, B.; Monnerie, L. *Adv. Polym. Sci*.**1994**, *116*, 145.

(34) Ediger, M. D.; Adolf, B. D. *Adv. Polym. Sci*. **1994**, *116*, 73.

(35) Moe, N. E.; Ediger, M. D. *Macromolecules* **1995**, *28*, 2329.

(36) Moe, N. E.; Ediger, M. D. *Macromolecules* **1996**, *29*, 5484.

(37) Fuson, M. M.; Ediger, M. D. *Macromolecules* **1997**, *30*, 5704.

(38) Fuson, M. M.; Hanser, K. H.; Ediger, M. D. *Macromolecules* **1997**, *30*, 5714.

(39) Horinaka, J.; Ito, S.; Yamamoto, M.; Matsuda, T. *Comput. Theor. Polym. Sci*. **2000**, *10*, 365.

(40) Horinaka, J.; Maruta, M.; Ito, S.; Yamamoto, M. *Macromolecules* **1999**, *32*, 1134.